Covalent and metallic bonding within the quasi-ion approach

C. Falter, H. Rakel, and W. Ludwig
Institut für Theoretische Physik II, Universität Münster, Wilhelm-Klemm-Strasse 10, D-4400 Münster, West Germany
(Received 8 February 1988)

A recently proposed theory of a quasi-ion description of solids is used to discuss simultaneously the dynamics of bonding and its relation to the phonon dispersion in crystals. The theory can be applied in principle to all types of bonding and allows a rigorous separation into "two-center" forces and proper many-body interactions. Applications for this separation are provided with respect to the metallic and covalent bonding type. In particular it is shown, using Si as an example, how angular rigidity of the covalent bond can be described by relative rotations of the quasi ions. In case of metallic bonding, special many-body effects leading to an anomalous phonon dispersion are investigated within a simple model.

I. INTRODUCTION

A considerable amount of progress in the quantum-mechanical description of electronic and lattice-dynamical properties of solids has been achieved by making feasible the density-functional theory of Hohenberg and Kohn[1] and of Kohn and Sham[2] by means of numerical procedures. On the other hand, the alternative route to these subjects, the density-response approach, as described by Pick, Cohen, Martin[3] and by Sham[4] is much more complicated to perform numerically.

On the basis of the density-response approach we recently have developed the quasi-ion (atom) description of solids.[5–9] In this theory the basic variable of the Hohenberg-Kohn theorem, i.e., the electronic density ρ, is further analyzed on a more elementary level. This leads to the quasi ions or partial densities from which the total density ρ can be reconstructed in a unique way. An important feature of these objects is their localization in space which allows a direct modeling of the electronic and lattice-dynamical properties of solids and of the electron-phonon interaction[8,9] as well.

Section II of this paper presents a condensed review of the construction of the quasi ions. Characteristic features are demonstrated for covalent and metallic bonding using Si and Na as examples. In Sec. III we are dealing with the bonding dynamics in a crystal in terms of quasi ions. The mechanism of angular rigidity of the covalent bond is described by special many-body forces in terms of rotations of the quasi ions and the corresponding effects on the phonon dispersion are studied. In case of metallic bonding a fictitious model system with an inhomogeneous electron distribution is constructed and effects related to the inhomogeneity are investigated.

II. QUASI IONS IN CRYSTALS

In the adiabatic approximation the electrons are regarded to follow the motion of the ions instantaneously at all frequencies. Thus, from a physical point of view it is easy to imagine that the electronic charge distribution of the ion core moves rigidly with the nucleus. In Refs. 5–9 it was shown that something similar occurs also with the valence electrons. The minimization of the change in energy of the system when an ion is displaced is physically achieved by an electronic density response in such a way that the displacement induced change of the ionic potential is self-consistently screened by the electrons. In this way the system is kept locally neutral. Figuratively this results in a displaced entity, the quasi ion, which consists of the ion core and a neutralizing distribution of screening charge surrounding it during its motion. It should be remarked that in general beside the rigid shift of the quasi ions also distortions of the charge distribution may occur during this polarization process. These are related to proper many-body forces and will be discussed in Sec. III.

Mathematically the unique decomposition of the valence charge density ρ into a superposition of partial or quasi-ion densities ρ_α can be achieved by the acoustic sum rule.[5–7] The result is represented in Fourier space and the limit $\mathbf{q}\rightarrow\mathbf{0}$ is implicitly understood:

$$\rho(\mathbf{q}+\mathbf{G})=\sum_\alpha \rho_\alpha(\mathbf{q}+\mathbf{G}) \underset{\mathbf{q}\rightarrow\mathbf{0}}{\rightarrow} \rho(\mathbf{G})=\sum_\alpha \rho_\alpha(\mathbf{G}) , \tag{1}$$

with

$$\rho_\alpha(\mathbf{q}+\mathbf{G})=-\frac{1}{4\pi}\sum_j v_{|j}(\mathbf{q}+\mathbf{G})^* \sum_{\mathbf{G}'} D(\mathbf{q}+\mathbf{G},\mathbf{q}+\mathbf{G}') \times V^\alpha_{|j}(\mathbf{q}+\mathbf{G}') , \tag{2}$$

$$V^\alpha_{|j}(\mathbf{q}+\mathbf{G})=-i(\mathbf{q}+\mathbf{G})_j V_\alpha(\mathbf{q}+\mathbf{G}) e^{-i\mathbf{G}\cdot\mathbf{R}^\alpha} , \tag{3}$$

$$v_{|j}(\mathbf{q})=-i\frac{4\pi}{q^2}q_j . \tag{4}$$

Here $\mathbf{q}$ is a vector from the first Brillouin zone and $\mathbf{G}$ a reciprocal-lattice vector. D describes the static density-response function (matrix) and V_α is the ionic pseudopotential corresponding to an ion of sublattice type α. The positions of the ions in the crystal are denoted by $\mathbf{R}^A=\mathbf{R}^{\mathbf{a}}+\mathbf{R}^\alpha$ or $\mathbf{A}=\mathbf{a}+\boldsymbol{\alpha}$ in short, where $\mathbf{a}$ and $\boldsymbol{\alpha}$ characterize the primitive and nonprimitive lattice vectors, respectively.

For a direct description of bonding and lattice dynamics it is suitable to express the quasi ions $\rho^{\mathbf{A}}$ in direct space. Correspondingly we obtain

$$\rho(\mathbf{r})=\sum_{\mathbf{A}}\rho^{\mathbf{A}}(\mathbf{r})=\sum_{\mathbf{A}}\rho_\alpha(\mathbf{r}-\mathbf{A})\ , \tag{5}$$

with

$$\rho^{\mathbf{A}}(\mathbf{r})=-\frac{1}{4\pi}\int dV'dV''\sum_j v_{|j}(\mathbf{r}-\mathbf{r}')D(\mathbf{r}',\mathbf{r}'')\times\frac{\partial}{\partial A_j}V_\alpha(\mathbf{r}''-\mathbf{A})\ , \tag{6}$$

$$v_{|j}(\mathbf{r}-\mathbf{r}')=\frac{\partial}{\partial r_j}v(\mathbf{r}-\mathbf{r}')=\frac{\partial}{\partial r_j}\frac{1}{|\mathbf{r}-\mathbf{r}'|}\ . \tag{7}$$

The decomposition of ρ within the above scheme clarifies the way which the quasi ions can be considered as new complex unities building up the crystal.

In Fig. 1 we have reproduced the contour plot of the Fourier transform of ρ_α in Si from Eq. (2) in the $(0,-1,1)$ plane. Figure 2 represents the superposition of the two sublattice partial densities ρ_α $(\alpha=1,2)$ yielding the total valence charge density ρ of Si. For the computational details we refer to Refs. 6 and 7. We deduce that as a consequence of the local-field effect, originating from the nondiagonal elements of the density-response function, the quasi ion ρ_α is highly anisotropic and inhomogeneous in the bond region and has locally tetrahedral symmetry. Furthermore, we observe a strong localization effect of the charge density neutralizing the ionic charge at short distances. The distribution is essentially confined to the bond region along the chains of Si atoms. This supports the conclusion that essential parts of the interactions between the ions can be described via anisotropic effective short-range force constants in phenomenological models. The largest extension of the forces is along the Si chains. This is in agreement with considerations given recently by Kane.[10] A more detailed inspection of the Si quasi ion demonstrates that in the bond directions at about $\frac{1}{3}$ of the bond length the density response is significantly enhanced leading to a very effective screening of the Coulomb potential of the ions at short distances. On the other hand, this "overscreening effect" gives rise to regions in space where the electrons are pushed away. In the interstitial region the density is nearly constant (flat) and approximately zero.

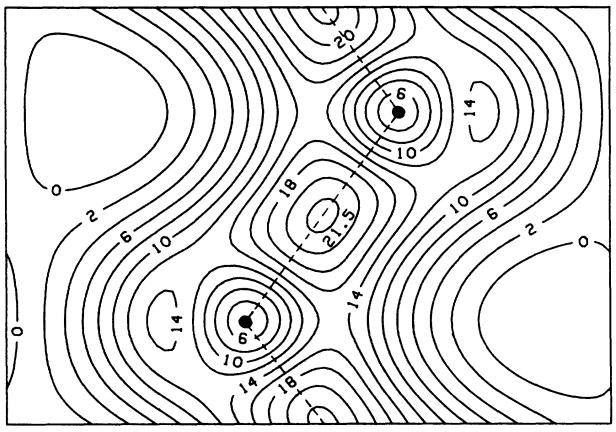

FIG. 2. Contour line plot of the valence charge density of Si in the $(0,-1,1)$ plane as calculated from the acoustic sum rule according to Eqs. (1)–(4). Units and labeling as in Fig. 1.

Next we show how the different types of bonding can be discussed in terms of their different screening properties. The latter are mapped as shown by Eqs. (2) and (6) via D to the quasi ions and thus bonding in solids is quite naturally displayed in direct space by these objects.

In the following we present an extract of our calculations recently performed for Na.[11] In this case (weak pseudopotential theory) it is sufficient to use linear screening with the response function of the homogeneous electron gas being diagonal in $\mathbf{q}$ space.[12,13] In order to calculate the sublattice partial density [Eq. (2)] in analogy to the Si case we artificially introduce a decomposition of the bcc structure into two simple-cubic sublattices centered at $\mathbf{R}^1=(0,0,0)$ and $\mathbf{R}^2=\frac{1}{2}a(1,1,1)$ (a denotes the lat-

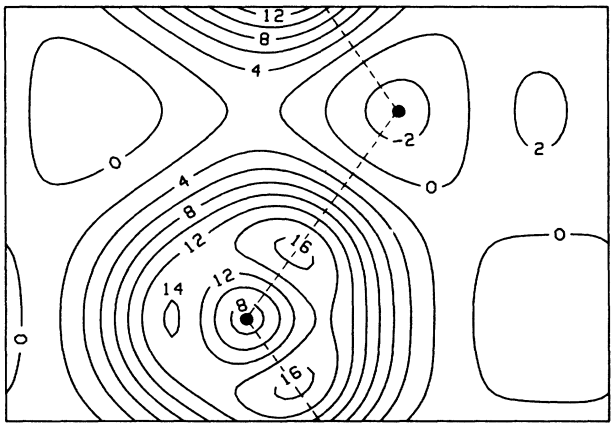

FIG. 1. Partial charge density $\rho_1(\mathbf{r})$ in the $(0,-1,1)$ plane for one sublattice of Si as calculated from Eqs. (2)–(4). ρ_1 is in units of electrons per cell. Ions are indicated as black dots and bonds by dashed lines.

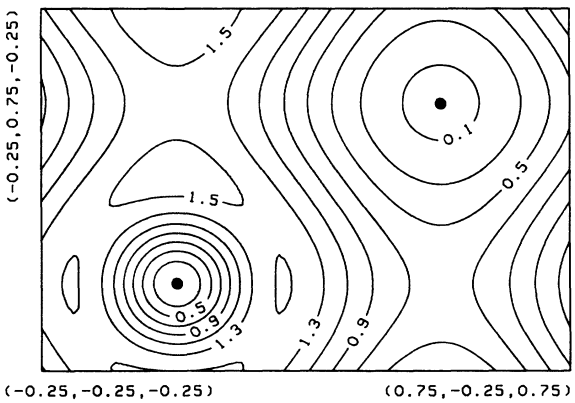

FIG. 3. Partial density of a sodium crystal in the $(-1,0,1)$ plane. Units are in electrons per (simple) cubic cell; coordinates are in units of the lattice constant a.

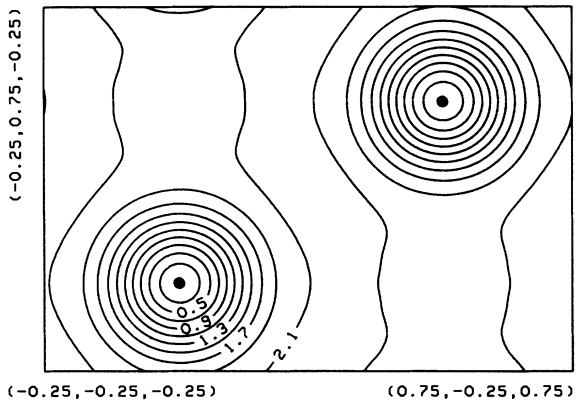

FIG. 4. Superposition of the two simple-cubic sublattice partial densities in the $(-1,0,1)$ plane centered at (0,0,0) and $(a/2)(1,1,1)$, respectively. Units and labeling as in Fig. 3.

tice constant). In Fig. 3 the results of the calculation are displayed as a contour line plot in the $(-1,0,1)$ plane. Figure 4 shows the corresponding superposition of the partial densities producing the total charge density of Na. In Figs. 5(a) and 5(b) we have represented the atomic partial density being of spherical shape because the density-response function is diagonal in $\mathbf{q}$ space. Apart from the long-range Friedel oscillations this density is remarkably well localized.

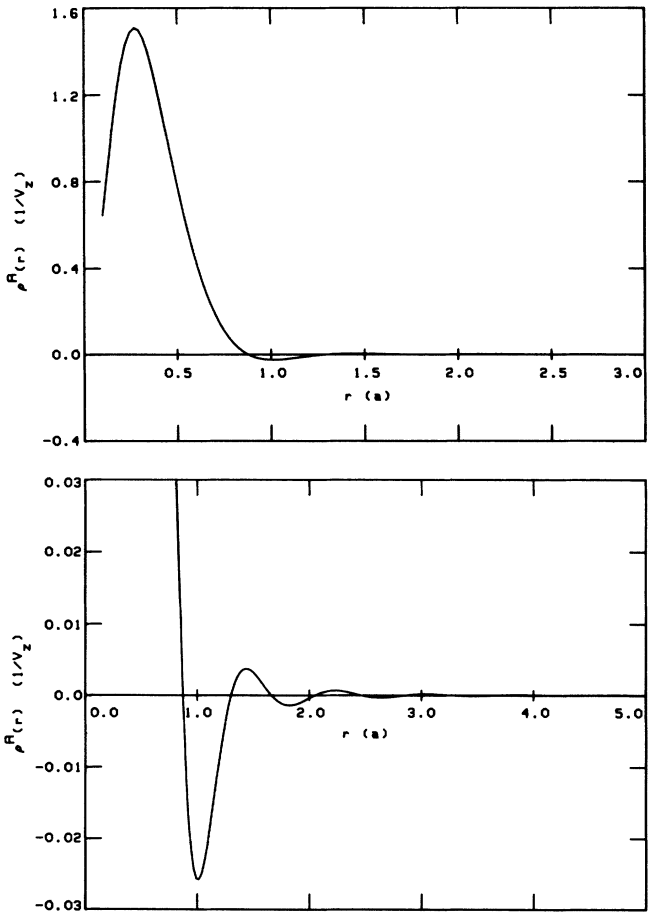

FIG. 5. (a) Atomic partial density $\rho^{A}(|\mathbf{r}|)$ for sodium normalized to 1. $|\mathbf{r}|$ is in units of the lattice constant a. (b) Same as in (a), but with a better resolution for $\rho^{A}(|\mathbf{r}|)$.

A comparison of the results for Na with those obtained for Si visualizes the qualitative differences of semiconductor screening and metallic screening. In case of Si localization is more strongly enhanced and we obtain a very inhomogeneous distribution with sharp maxima and minima which is confined to the bond region along the Si chains. On the other hand Na displays a more smooth but nevertheless localized sublattice partial density. No maxima appear along the directions towards nearest neighbors. However weak maxima evolve towards second and third neighbors and it seems to be remarkable that one can obtain with the structured partial density of Fig. 3 a nearly structureless total density corresponding, of course, to the Fermi-gas picture of the electrons in a simple metal.

We conclude this section by noting that the quasi-ion approach allows also for a direct application to lattice dynamics.[7-9] In its simples version (rigid quasi-ion approximation) the knowledge of the partial density and the ionic pseudopotential alone are sufficient. In the following section we shall discuss this matter in more detail.

III. BOND DYNAMICS AND PHONON DISPERSION IN TERMS OF QUASI IONS

The basic quantity which contains all the relevant information for microscopic lattice dynamics in harmonic approximation is the vector field[7-9]

$$P_j^{\mathbf{A}}(\mathbf{r})=P_j^{\alpha}(\mathbf{r}-\mathbf{A})=\int dV' D(\mathbf{r},\mathbf{r}')\frac{\partial}{\partial A_j}V_{\alpha}(\mathbf{r}'-\mathbf{A}) ,$$

or (8)

$$P_j^{\mathbf{A}}=DV_{|j}^{\mathbf{A}} ,$$

in a compact notation. This field has the meaning of the charge-density variation at the space point $\mathbf{r}$ produced by a unit displacement of ion $\mathbf{A}$ in direction j. From its knowledge we can compute all the relevant quantities as the total charge-density variation $\delta\rho$ and the electron mediated part Λ_E of the dynamical matrix. The corresponding expressions are given in Refs. 6–9.

Following these references, the quasi-ion picture can be used for the decomposition of $\mathbf{P}^{\mathbf{A}}(\mathbf{r})$ into a rigid and a distortion part. This is achieved by decomposing $\mathbf{P}^{\mathbf{A}}(\mathbf{r})$ into a gradient and a rotational (distortion) contribution

$$\mathbf{P}^{\mathbf{A}}(\mathbf{r})=\nabla\rho^{\mathbf{A}}(\mathbf{r})+\nabla\times\mathbf{W}^{\mathbf{A}}(\mathbf{r}) . \quad (9)$$

For such a decomposition see also Ball[14] and Pickett.[15]

The $\rho^{\mathbf{A}}(\mathbf{r})$ are just the quasi ions defined in Eq. (6) and represent the rigid part of the density variation while the distortion is described by the curl of the vector field $\mathbf{W}^{\mathbf{A}}$, see Refs. 7–9 for more details. From Eqs. (6) and (9) it is then obvious that the density which moves rigidly with the ion is not determined alone by the ion itself but depends implicitly via D on *all* the ions in the crystal. The investigations[7] for Si have shown that the charge redistri-

bution and the phonon dispersion are quite well described by the rigid part indicating that an approximative description of lattice dynamics in terms of rigid quasi ions provides a promising starting point. The influence of the distortions turned out to be relatively small for most of the phonon modes. However, for certain modes and at some particular points in the Brillouin zone the distortions play a more important role. Particularly for the transverse acoustic (TA) mode the distortion term produces a lowering of the calculated phonon frequencies. Furthermore, in case of the transverse optical (TO) (Γ)-phonon–induced charge-density variation we extract a non-negligible contribution to the interbond charge transfer, due to the distortions.[7] Yet, this additional nonrigid charge transfer seen in the TO (Γ)-phonon has no influence on the phonon frequency at Γ for symmetry reasons.

If only rigid nonspherical quasi ions are taken into account this approximation is equivalent to using "two-center forces" which reduce to central forces for spherical densities like in Na. On the other hand proper many-body forces can be introduced into the quasi-ion description by considering the distortion part of $\mathbf{P}^{\mathbf{A}}(\mathbf{r})$. This can be done by relating the charge-density variation $\mathbf{P}^{\mathbf{A}}$ induced by displacing ion **A** to the positions of the neighboring ions. In this way the violation of rotational invariance caused by rigid nonspherical quasi ions can also be restored. In the following we rewrite the vector field from Eq. (9) in the form

$$\mathbf{P}^{\mathbf{A}}(\mathbf{r})=\nabla\rho^{\mathbf{A}}(\mathbf{r})+\mathbf{P}_d^{\mathbf{A}}(\mathbf{r}) , \tag{10}$$

where $P_d^{\mathbf{A}}$ stands for the distortion contribution. For a representation of this part, i.e., for an extension of the rigid quasi-ion description, we will allow for specific assumptions. We shall investigate two types of distortions. One contribution to $\mathbf{P}_d^{\mathbf{A}}$ is constructed by admitting rigid rotations of the quasi ions ($\mathbf{P}_r^{\mathbf{A}}$) and the second one by allowing for a contraction or expansion, i.e., breathing ($\mathbf{P}_b^{\mathbf{A}}$).

The definite representation of these effects is performed in such a way that translational and rotational invariance of the system is maintained, i.e.,

$$\sum_{\mathbf{A}} \mathbf{P}_d^{\mathbf{A}}(\mathbf{r})=0 \tag{11}$$

and

$$\sum_{\mathbf{A}} [(\mathbf{A}-\mathbf{r})\times\mathbf{P}^{\mathbf{A}}(\mathbf{r})]=0 . \tag{12}$$

The mathematical realization of the models in the case of rotations is accomplished by calculating first the charge-density variation $\delta\rho^{\mathbf{B}}$ which arises from a rotation of the quasi ion at **B** when ion **A** is displaced,

$$\delta\rho^{\mathbf{B}}(\mathbf{r})=\Phi(|\mathbf{A}-\mathbf{B}|)\times\left[\frac{(\mathbf{A}-\mathbf{B})}{|\mathbf{A}-\mathbf{B}|^2}\times[(\mathbf{r}-\mathbf{B})\times\nabla\rho^{\mathbf{B}}(\mathbf{r})]\right]\cdot\mathbf{u}^{\mathbf{A}} . \tag{13}$$

Here $\Phi(|\mathbf{A}-\mathbf{B}|)$ is a parameter which describes a damping of the rotation and which is essential in order to satisfy the requirement of rotational invariance expressed by Eq. (12). If only nearest-neighbor rotations are taken into account this parameter is uniquely determined by this condition. The total density variation which is induced by rotations of the surrounding ions **B** when **A** is displaced then follows as

$$\delta\rho^{\mathbf{A}}(\mathbf{r})=\sum_{B\in S(\mathbf{A})}\delta\rho^{\mathbf{B}}(\mathbf{r})=\mathbf{P}_r^{\mathbf{A}}\cdot\mathbf{u}^{\mathbf{A}} , \tag{14}$$

with

$$\mathbf{P}_r^{\mathbf{A}}(\mathbf{r})=\sum_{B\in S(\mathbf{A})}\Phi(|\mathbf{A}-\mathbf{B}|)\times\left[\frac{(\mathbf{A}-\mathbf{B})}{|\mathbf{A}-\mathbf{B}|^2}\times[(\mathbf{r}-\mathbf{B})\times\nabla\rho^{\mathbf{B}}(\mathbf{r})]\right] . \tag{15}$$

The second type of distortions considered here are those of breathing type. A displacement $\mathbf{u}^{\mathbf{A}}$ parallel to the axis joining ion **A** and **B** cannot generate rotations of the quasi ions. But an additional charge-density variation can occur in comparison with the variation induced by the rigid shift of the quasi ions if the latter are allowed to expand or to contract. This effect is also present in the case of spherical quasi ions (simple metals) where rotations are ineffective. In our model we treat it by a suitable scaling of the quasi ions. The charge-density variation induced by breathing of the neighbors of a given ion **A** is then represented by

$$\delta\rho^{\mathbf{A}}(\mathbf{r})=\sum_{B\in S(\mathbf{A})}[\eta_{\mathbf{B}}^3\rho^{\mathbf{B}}(\eta_{\mathbf{B}}\mathbf{r})-\rho^{\mathbf{B}}(\mathbf{r})] , \tag{16}$$

where $\eta_{\mathbf{B}}$ is linear in $\mathbf{u}^{\mathbf{A}}$,

$$\eta_{\mathbf{B}}=1+\frac{(\mathbf{A}-\mathbf{B})}{|\mathbf{A}-\mathbf{B}|^2}\eta(|\mathbf{A}-\mathbf{B}|)\cdot\mathbf{u}^{\mathbf{A}} . \tag{17}$$

Finally, we obtain for the corresponding vector field of breathing type

$$\mathbf{P}_b^{\mathbf{A}}(\mathbf{r})=\sum_{B\in S(\mathbf{A})}\eta(|\mathbf{A}-\mathbf{B}|)\times\left[\frac{(\mathbf{A}-\mathbf{B})}{|\mathbf{A}-\mathbf{B}|^2}[3\rho^{\mathbf{B}}(\mathbf{r})+(\mathbf{r}-\mathbf{B})\cdot\nabla\rho^{\mathbf{B}}(\mathbf{r})]\right] . \tag{18}$$

In a real-space picture these nonrigid contributions of the charge-density variation correspond to quasi ions that lose their fixed shape and size according to the change of the local environment.

From our microscopic calculations for Si within the density-response approach in Ref. 7 it can be seen that the phonon-induced charge-density variations as well as the corresponding phonon frequencies are described quite well within the rigid quasi-ion approximation. Thus, we conclude that charge relaxation tends to preserve the tetrahedral quasi-ion configuration and so it is natural to include distortion contributions in the form of rotations via $\mathbf{P}_r^{\mathbf{A}}$. For the bond dynamics this means that the angular rigidity of the bond is determined by the relative rotations of the quasi ions leading to a deviation from collinearity of the two partial densities participating in a

common bond. This is in contradiction with the well-known valence force model. See, e.g., Ref. 16 where angular rigidity is related to a change of the bond angle between adjacent bonds while the bond remains straight. Our reasonings concerning rigid rotations point into a similar direction as a discussion recently given by Kane.[10]

We now give a quantitative investigation of the effect of $\mathbf{P}_r^{\mathbf{A}}$, i.e., of this special type of a three-body interaction, on the phonon dispersion in Si. For the model construction of the quasi-ion density $\rho_\alpha(\mathbf{r})$ we use the model explained in Ref. 7:

$$\rho_\alpha(\mathbf{r})=\sum_{\nu,\lambda}\left[\frac{\gamma_{\nu\lambda}^{\alpha}}{\pi}\right]^{3/2} C_{\nu\lambda}^{\alpha} e^{-\gamma_{\nu\lambda}^{\alpha}(\mathbf{r}-\mathbf{R}_{\nu\lambda}^{\alpha})^2} . \tag{19}$$

This leads to the phonon dispersion in the $\Delta=[1,0,0]$ direction as reproduced in Fig. 6. The ionic pseudopotential is taken to be the Appelbaum-Hamann potential.[17]

In expanding the quasi-ion density into a sum of ansatz functions as in Eq. (19) we benefit from the good localization properties of the quasi ions generated by the self-consistent screening mechanisms as already mentioned in Sec. II. Consequently, the partial densities can be expanded in terms of a well-localized set of basis functions (three Gaussians centered at an ion and another three centered at each of the four bonds in our model). This is crucial for numerical calculations. This feature of strong localization is similar to the self-consistent Green's-function method[18,19] where the defect induced density change $\Delta\rho$ is well localized in real space and only a highly localized basis set of functions is necessary for an expansion. Comparing the results for $\Delta\rho$, as obtained in Refs. 18 and 19 for the unrelaxed Si vacancy, with the result from Fig. 1 for the quasi ion in Si shows apparently a great similarity ($\Delta\rho\approx-\rho^{\mathbf{A}}$).

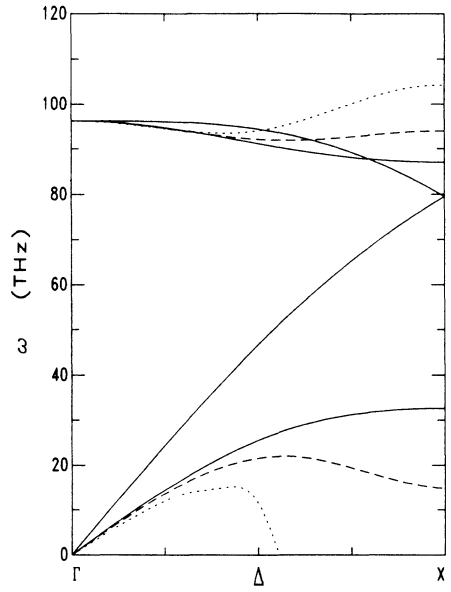

FIG. 7. Phonon dispersion curves $\omega(\mathbf{q})$ along the Δ direction in Si within the rigid quasi-ion approximation (solid curves). The dashed ($\Phi=2a^{-2}$) and dotted curves [$\Phi=(16/3)a^{-2}$] result if distortions of the quasi ions in form of nearest-neighbor rotations are taken into account.

Using the quasi-ion density of Eq. (19) in Eqs. (10) and (15) we can calculate after Fourier transformation the electronic contribution Λ_E to the dynamical matrix. The results for several calculations including distortions of ro-

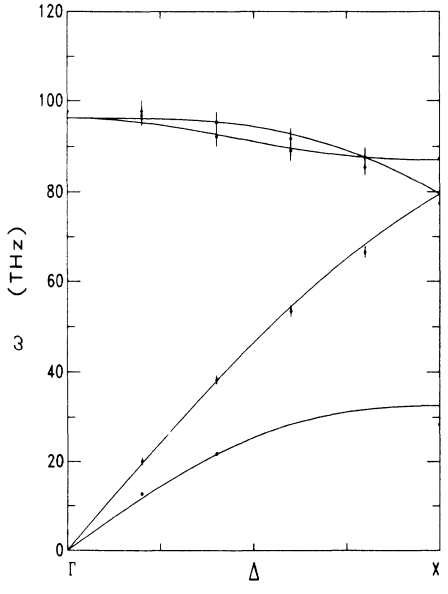

FIG. 6. Phonon dispersion curves $\omega(\mathbf{q})$ for Si along the $\Delta\|[1,0,0]$ direction as calculated from the rigid quasi-ion model (Ref. 7). The barred dots indicate the experimental data including error.

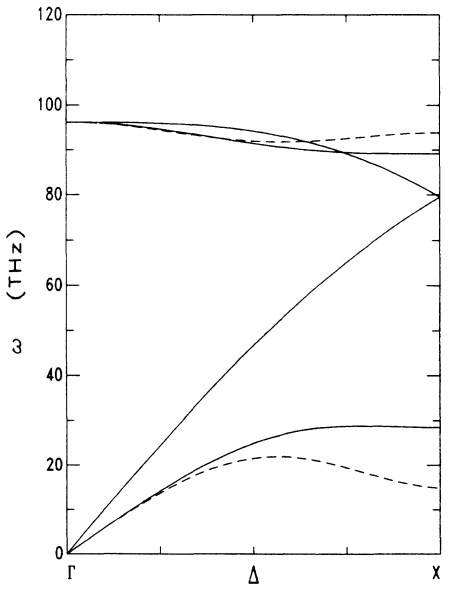

FIG. 8. Phonon dispersion of Si along the Δ direction using first- (dashed curves) and first- and second-neighbor rotations (solid curves).

tation type are shown in Figs. 7–9 for Si in the $\Delta=[1,0,0]$ direction.

First of all we notice that phonon modes other than the TA mode are less (TO) or not at all influenced by these type of three-body forces. In Fig. 7 we consider nearest-neighbor rotations only. The broken curves were obtained fixing $\Phi(=2a^{-2})$ in Eq. (15) by the condition of rotational invariance [Eq. (12)]. The solid lines represent the rigid quasi-ion model, $\Phi=0$, while the dotted curves are calculated with $\Phi=16/(3a^2)$ corresponding to a rigid undamped rotation. As a result, we extract from these investigations that a decrease of the rigidity of the quasi ions during rotations, characterized by increasing Φ values, leads in a first step to a decrease and flattening of the TA dispersion ($\Phi=2a^{-2}$) and finally to a softening [$\Phi=16/(3a^2)$] of this mode. Figures 8 and 9 demonstrate the effect of second-neighbor rotation contributions on the phonon frequencies. The broken curves in Fig. 8 are as before the dispersions curves for nearest-neighbor rotations with $\Phi=2a^{-2}$, while the solid curves are the results from a calculation taking into account second-neighbor rotations. The main effect of the latter is a stabilization of the TA frequencies without destroying the flattening of the dispersion. Compare also with Fig. 9 where the comparison with the rigid quasi-ion model ($\Phi=0$) is given.

Next we discuss possible effects of three-body contributions of breathing type, Eq. (18), on the phonon dispersion. Because this type of a many-body interaction could also be present for spherical partial densities we have studied here the case of metallic bonding using Na as an example. In Ref. 11 we also have investigated a charge-density distribution of a hypothetical system which is intended to represent directional bonding originating from localized (d) electrons. This type of bonding is very important for a description of the vibrations of the ions in the transition metals.[20,21] See Ref. 11 for more details, especially as far as the effects of the rotations of the quasi ions are concerned.

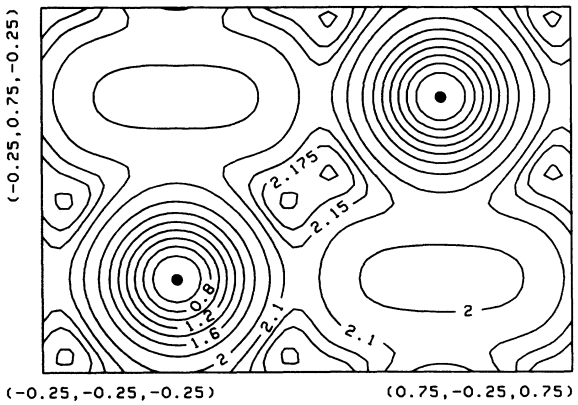

FIG. 10. Contour plot in the $(-1,0,1)$ plane of the valence charge density of the hypothetical system consisting of nonspherical quasiatoms as discussed in the text. Units and labeling as in Fig. 3.

In Fig. 10 the contour line plot of the valence charge density of such a hypothetical system with nonspherical quasiatoms is shown in the $(-1,0,1)$ plane. Here we have assumed that 5% of the total density is ascribed to the nonspherical part. The density should be compared with Fig. 4 where the corresponding charge density of Na using spherical quasiatoms is shown. The main effect derived from the anisotropic part of the quasiatom consists in a more inhomogeneous electron distribution with an increase of the density in the region between nearest neighbors. This leads to an elongated shape with two weak maxima and thus gives rise to weak directional bonding. In addition more charge is contracted in the neighborhood of the ions. Such a kind of charge redistri-

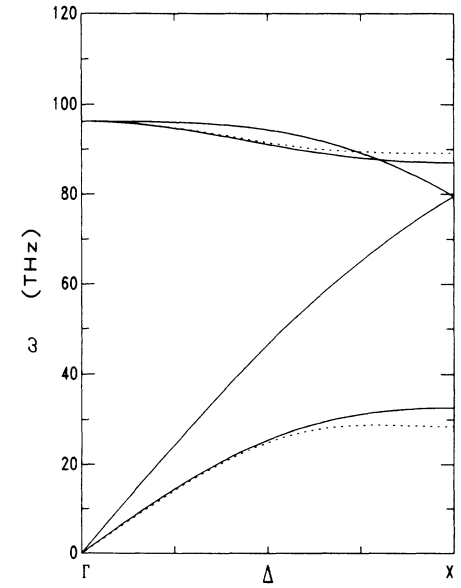

FIG. 9. Comparison of the phonon dispersion of Si in the rigid quasi-ion approximation (solid curves) with a calculation including first- and second-neighbor rotations (dotted curves).

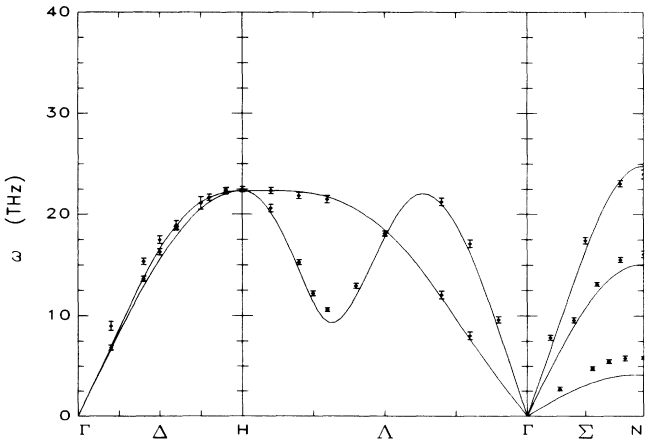

FIG. 11. Phonon dispersion of Na along the main symmetry directions as calculated on the basis of spherical quasiatoms. The calculation is performed by approximating the quasiatom density displayed in Fig. 5 with three Gaussians only. The barred dots indicate the experimental data including error.

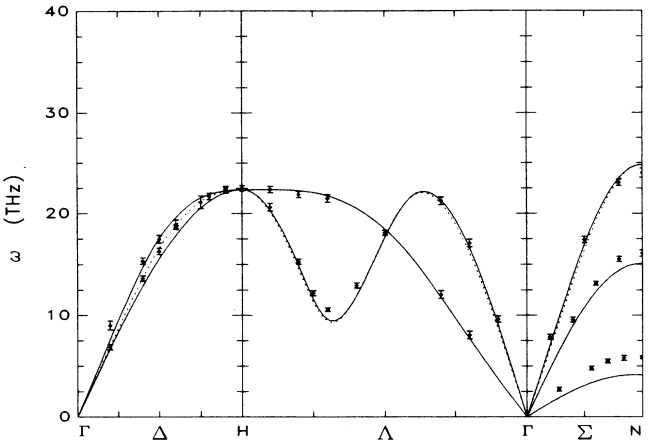

FIG. 12. Illustration of the breathing effect of spherical quasiatoms on the phonon dispersion of Na (solid curves). For reference the results from the rigid quasiatoms are also drawn (dotted curves). The barred dots represent the experimental data including error.

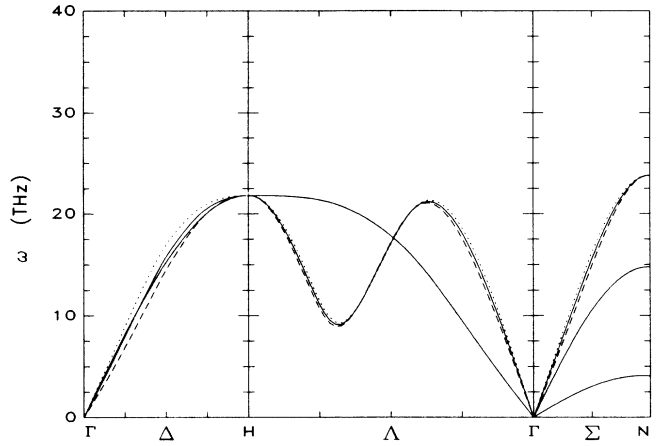

FIG. 14. Phonon dispersion in the main symmetry directions for our hypothetical system including breathing effects from the anisotropic quasiatoms. Solid curves are the reference curves for the rigid but anisotropic quasiatoms while dashed and dotted curves correspond to opposite breathing corrections $\eta=-0.03$ and $\eta=+0.03$, respectively.

bution allows for a more effective screening of the Coulomb interaction between the ions and it is an interesting question of how these features are reflected in the phonon dispersion.

Just as in the case of Si the spherical quasiatoms of Na shown in Figs. 5(a) and 5(b) are approximated by Gaussian ansatz functions as given in Eq. (19). The results for the phonon dispersion of such a model calculation based on rigid quasi ions are displayed in Fig. 11 where only three Gaussians have been taken into account. We extract from these calculations that the description of lattice dynamics of simple metals with rigid and spherical quasiatoms is in good agreement with experiment.

The breathing effect of the spherical quasiatoms on the phonon dispersion of Na can be extracted from Fig. 12. For comparison the frequencies as obtained from the rigid quasiatom model as calculated with three ansatz Gaussians are also drawn (dotted curves). The breathing parameter η was taken to be $\eta=-0.024$ and only nearest-neighbor breathing was considered. The breathing corrections act on the longitudinal modes only and lead to a slight improvement of the longitudinal-acoustic-phonon frequencies.

In Figs. 13–15 phonon dispersion curves for bcc structure based on our nonspherical fictitious quasiatoms are presented. The results of a calculation using the anisotropic but rigid quasi ions are displayed in Fig. 13 and are compared with the rigid isotropic quasi ion results from Fig. 11 (dotted curves). We realize a lowering of the whole phonon spectrum which can be attributed by this calculation to the inhomogeneous redistribution of charge and a more effective screening between the ions as

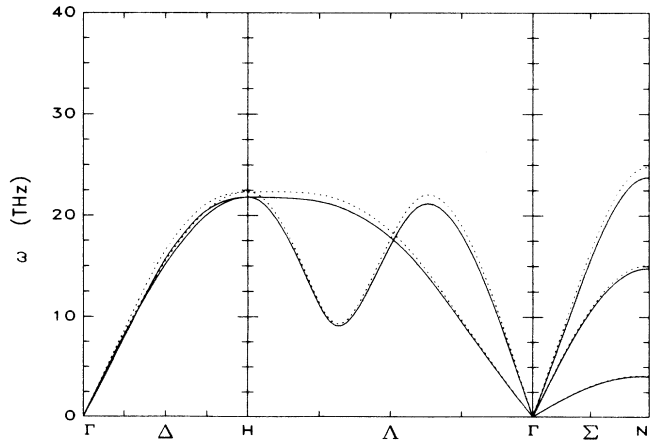

FIG. 13. Comparison of the phonon dispersion as calculated from the anisotropic but rigid quasiatom (solid curves) with the corresponding curves as obtained with the rigid isotropic quasiatom from Fig. 11.

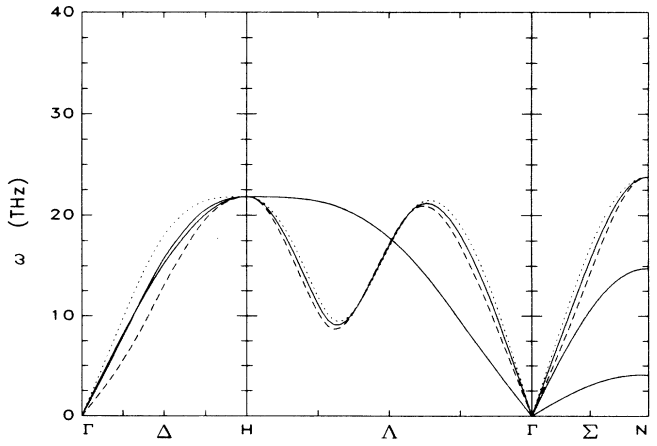

FIG. 15. Same as in Fig. 14 but with an increased breathing contribution ($\eta=\pm0.06$).

discussed in context with Fig. 10. Finally, the effect of the many-body corrections of anisotropic breathing on the phonon dispersion can be read off from Figs. 14 and 15. Solid curves result from the rigid but anisotropic quasi ion while dotted and dashed curves include breathing with $\eta=0.03$ (Fig. 14), $\eta=0.06$ (Fig. 15), $\eta=-0.03$ (Fig. 14) and $\eta=-0.06$ (Fig. 15), respectively. The most remarkable effect which is brought about by this many-body force related to anisotropic quasi-ion breathing is that characteristic and anomalous structures now appear in contrast to the featureless phonon dispersion of the simple metals. We obtain phonon stiffening and phonon softening which is very similar to what is observed in *d*-electron metals.[20–24] Thus, despite the fact that we are dealing with investigations of a fictitious model system the results of our calculation lead to the conjecture that the anomalous behavior in the phonon dispersion of the *d*-electron metals should be related to the distortion part of the vector field $\mathbf{P}^{A}$ and consequently to many-body interactions which may be modeled in terms of the quasi ions.

ACKNOWLEDGMENTS

We would like to thank Dr. M. Selmke, Dr. A. Mayer, Dr. W. Zierau, and M. Klenner for useful discussions. Support by the Deutsche Forschungsgemeinschaft (Bonn, Germany) Project No. FA-170/1-2 is gratefully acknowledged.

[1]P. Hohenberg and W. Kohn, Phys. Rev. **136**, 864 (1964).
[2]W. Kohn and L. J. Sham, Phys. Rev. **140**, A1133 (1965).
[3]R. M. Pick, M. H. Cohen, and R. M. Martin, Phys. Rev. B **1**, 910 (1970).
[4]L. J. Sham, Phys. Rev. **188**, 1431 (1969).
[5]C. Falter, W. Ludwig, M. Selmke, and W. Zierau, Phys. Lett. **105A**, 139 (1984).
[6]C. Falter, W. Ludwig, A. A. Maradudin, M. Selmke, and W. Zierau, Phys. Rev. B **32**, 6510 (1985).
[7]C. Falter, M. Selmke, W Ludwig, and K. Kunc, Phys. Rev. B **32**, 6518 (1985).
[8]C. Falter, W. Ludwig, M. Selmke, and W. E. Pickett, J. Phys. C **20**, 501 (1987).
[9]C. Falter, Phys. Rep. (to be published).
[10]E. O. Kane, Phys. Rev. B **31**, 7865 (1985).
[11]H. Rakel, C. Falter, and W. Ludwig (unpublished).
[12]J. M. Ziman, Adv. Phys. **13**, 89 (1964).
[13]C. Falter, W. Ludwig, W. Zierau, and M. Selmke, Phys. Lett. **93A**, 298 (1983).
[14]M. A. Ball, J. Phys. C **8**, 3328 (1975); **10**, 4921 (1977); **15**, 229 (1982).
[15]W. E. Pickett, J. Phys. C **12**, 1491 (1979).
[16]H. L. McMurry, A. W. Solbrig, Jr., J. K. Boyter, and C. Noble, J. Phys. Chem. Solids **28**, 2359 (1967).
[17]J. A. Appelbaum and D. R. Hamann, Phys. Rev. B **8**, 1777 (1973).
[18]J. Bernholc, N. O. Lipari, and S. Pantelides, Phys. Rev. B **21**, 3545 (1980).
[19]G. A. Baraff and M. Schlüter, Phys. Rev. B **19**, 4965 (1979).
[20]K. M. Ho, C. L. Fu, and B. N. Harmon, Phys. Rev. B **28**, 6687 (1983).
[21]K. M. Ho, C. L. Fu, and B. N. Harmon, Phys. Rev. B **29**, 1575 (1984).
[22]Y. Chen, K. M. Ho, B. N. Harmon, and C. Stassis, Phys. Rev. B **33**, 3684 (1986).
[23]J. A. Moriarty, Phys. Rev. Lett. **55**, 1502 (1985).
[24]J. A. Moriarty, Phys. Rev. B **34**, 6738 (1986).